Preliminary numerical computations in the context of imaging for conductivity defects

R. Condori[a], J. De Sousa[a], I. Mannarino[a], J. Parada[a], L.F. Plaza[a], F.A. Sequeira[a]

[a] *Research School, CIMPA, University of Simón Bolívar, 2012.*

Abstract

The aim of this work is to illustrate numerically the detection of a single conductivity defect in a bounded domain by making use of an approach based on the Electrical Impedance Tomography (EIT) method [1]. From a practical point of view, such a defect could represent a breast cancer tumor. A simple implementation for the detection is achieved using `FreeFem++` and `Scilab` for computations.

Keywords: conductivity defects, finite element methods, numerical approximations, `FreeFem++`, `Scilab`

1. Introduction

As we know, cancer is an accelerated and disorderly growth of malignant cells in a tissue of an organ. In this project, we refer more specifically to breast cancer. To detect the accumulation of cells that this process originates, exists two principally methods: mammography and ultrasound. Both techniques can be expensive, and in some cases, both omit small tumors not visible, or create false results of presence of tumor (false positives). To avoid this last disadvantage, were created new procedures to locate the possible tumor; one of this is the EIT (Electrical Impedance Tomography).

The EIT is a process where are generated images of the distributions of opposition or resistance which presents the cells to the pass of electricity, when a voltage is applied to the body of the patient. That is, the EIT is a method that consists in introduced voltage to the human body to generate images of the structures where are changes in the electrical current. These changes can be observed or detected because the normal and cancer cells have different conductivities.

The electric circuit structure is characterized by the location of the nodes through which is introduced and leaved the current: foot and breast, respectively. Furthermore, this system is connected to a computer which scans the circuit behavior. When the current enters to the body, it travels to the breast, where is measured the difference in conductivities, and

Email addresses: `raul_condori@hotmail.com` (R. Condori), `jessica.de.sousaf@gmail.com` (J. De Sousa), `antonella78@hotmail.com` (I. Mannarino), `jaime.parada@gmail.com` (J. Parada), `lplaza@uceva.edu.co` (L.F. Plaza), `f.sequeir@una.ac.cr` (F.A. Sequeira)

then, if presents a discrepancy, the computer generates the image of the tumor, in order to locate it through the mathematical model.

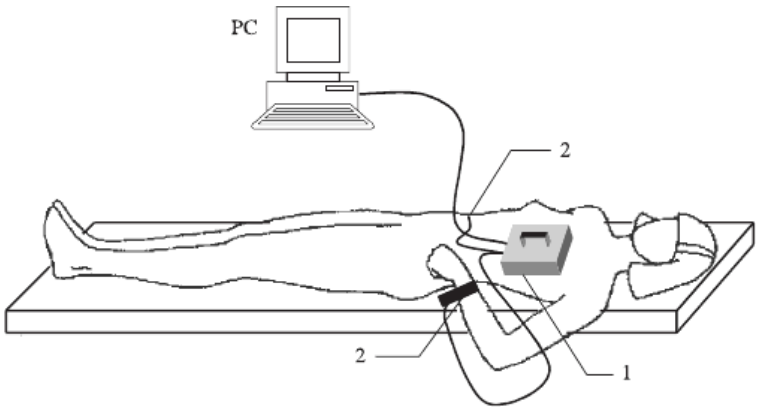

Figure 1: System and measuring procedure

2. The model problem

The problem of determining interior information about a medium from boundary field measurements is one that is not in general well posed. If, however, in advance we have additional structural information about the medium, then we may be able to determine specific features with "higher resolution", [1].

Let Ω be a bounded open subset of $\mathbb{R}^2$, with a smooth boundary denoted by $\partial\Omega$, and containing an inhomogeneity D. We assume that this inhomogeneity is small and consider

$$D \;=\; z + \varepsilon B,$$

where $B \subset \mathbb{R}^2$ is a ball containing the origin (this if for easy mathematical computations), $z \in \mathbb{R}^2$ denotes the "location" of the inhomogeneity, o represents the order of magnitude of the inhomogeneity and is taken sufficiently small when compared to the diameter of Ω. We also assume that $\text{dist}(z, \partial\Omega) \geq d_0 > 0$, with d_0 a fixed constant.

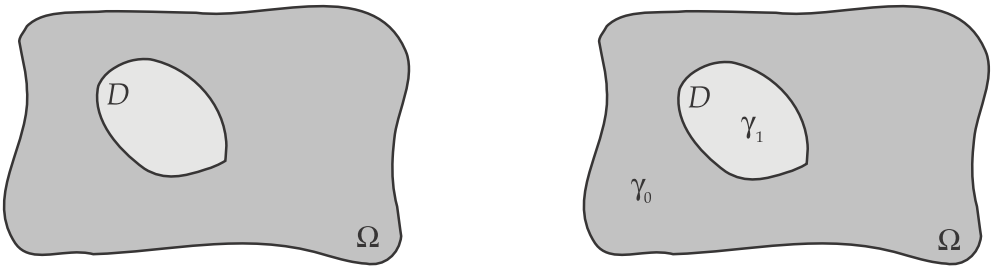

Figure 2: Idea of Ω (left) and the conductivity (right)

Let us set, for $x \in \overline{\Omega}$,

$$\gamma_\varepsilon(x) \;=\; \begin{cases} \gamma_0 & \text{if} \quad x \in \overline{\Omega} \setminus \overline{D}, \\ \gamma_1 & \text{if} \quad x \in D, \end{cases}$$

where γ_0, $\gamma_1 \in \mathbb{R}$, $\gamma_1 > \gamma_0 > 0$. The parameter γ_ε allows us to describe the conductivity of the medium Ω, with γ_0 denoting the conductivity of $\overline{\Omega} \setminus \overline{D}$ and γ_1 that of D. Note that γ_ε is a discontinuos function and for that reason, it is not necessary to be defined on ∂D.

Now for the current, let $g \in H^{-\frac{1}{2}}(\partial\Omega)$ such that $\int_{\partial\Omega} g d\sigma = 0$ (this is for the existence of the solution of (1)), and let ν denote the outward unit normal to Ω. We consider the problem which consists of finding a function u_ε, defined in Ω, such that:

$$\begin{cases} -\mathrm{div}(\gamma_\varepsilon \mathrm{grad} u_\varepsilon) &=& 0 & \text{in } \Omega, \\ \gamma_\varepsilon \dfrac{\partial u_\varepsilon}{\partial \nu} &=& g & \text{on } \partial\Omega \\ \int_{\partial\Omega} u_\varepsilon d\sigma &=& 0. \end{cases} \tag{1}$$

In the absence of the inhomogeneity D, the potential satisfying the corresponding background problem is denoted by u_0, i.e., u_0 is the solution of the alternative problem:

$$\begin{cases} -\gamma_0 \Delta u_0 &=& 0 & \text{in } \Omega, \\ \gamma_0 \dfrac{\partial u_0}{\partial \nu} &=& g & \text{on } \partial\Omega \\ \int_{\partial\Omega} u_0 d\sigma &=& 0. \end{cases}$$

and for the Neumann boundary condition we can define the current g in terms of the potential u_0. In practice, we will have two potentials $u_0^{(1)}$ and $u_0^{(2)}$, and for that reason we will have two currents.

When we have the solution u_ε of (1), we can consider the measurement:

$$\Gamma \;:=\; \int_{\partial\Omega} u_\varepsilon \gamma_0 \frac{\partial w}{\partial \nu} d\sigma - \int_{\partial\Omega} g w d\sigma \tag{2}$$

where the current g is associated with u_ε as well as with u_0, and w is some (known) harmonic function. In order to evaluate certain measurements, we defined from (2) the following quantities,

$$\Gamma_{ij} \;:=\; \int_{\partial\Omega} u_\varepsilon^{(i)} \gamma_0 \frac{\partial w^{(j)}}{\partial \nu} d\sigma - \int_{\partial\Omega} g^{(i)} w^{(j)} d\sigma,$$

where $i = 1, 2$, $j = 1, 2, 3$, $u_0^{(i)}(x_1, x_2) = x_i$, $w^{(1)}(x_1, x_2) = u_0^{(1)} = x_1$, $w^{(2)}(x_1, x_2) = u_0^{(2)} = x_2$, and $w^{(3)}(x_1, x_2) = u_0^{(1)} u_0^{(2)} = x_1 x_2$.

Let us introduce the response matrix

$$R \;=\; \begin{pmatrix} \Gamma_{11} & \Gamma_{21} \\ \Gamma_{12} & \Gamma_{22} \end{pmatrix},$$

as well as the matrix equation

$$\begin{pmatrix} \Gamma_{13} \\ \Gamma_{23} \end{pmatrix} = R \begin{pmatrix} z_1 \\ z_2 \end{pmatrix} \tag{3}$$

where z_1 and z_2 are two real unknowns (components of the "location" z). The 2×2 linear system (3) provides us with the position of inhomogeneity D.

3. Finite element discretization

Let $\mathcal{T}_h$ a triangulation of Ω, the weak formulation of the problem (1) is obtained by multiplying the differential equation by test functions v_h in a finite-dimensional space $\in \mathcal{V}_h$ and then integrate by parts in Ω, where we obtain the following weak formulation:

$$\int_\Omega \gamma_\varepsilon \nabla u_h \cdot \nabla v_h = \oint_{\partial\Omega} g v_h, \quad \text{for all } v_h \in \mathcal{V}_h \tag{4}$$

$$\oint_{\partial\Omega} u_h = 0, \tag{5}$$

where $\mathcal{V}_h = \left\{ v : v \text{ continuous in } \Omega, \frac{\partial v}{\partial x} \text{ and } \frac{\partial v}{\partial y} \text{ piecewise continuous in } \Omega \right\}$, when first orden of approximation is used. Besides, $u_h \in \mathcal{V}_h$ is the orthogonal projection of u_ε on $\mathcal{V}_h$.

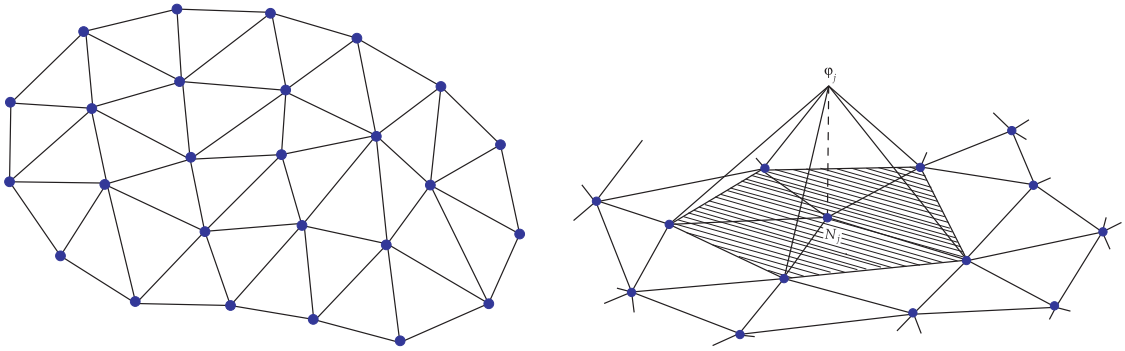

Figure 3: Example of: triangulation $\mathcal{T}_h$ (left) and finite space $\mathcal{V}_h$ (right)

Consider $\Phi = \{\varphi_i\}$ a basis for $\mathcal{V}_h$, and $\mathbf{u} = (u_i)$ the vector of coefficients such that

$$u_h(x) = \sum_{j=0}^{\dim(\mathcal{V}_h)} u_j \varphi_j(x), \quad \text{for } x \in \Omega. \tag{6}$$

and replacing v_h by φ_i in (4) we have

$$\int_\Omega \gamma_\varepsilon \nabla u_h \cdot \nabla \varphi_i = \oint_{\partial\Omega} g \varphi_i,$$

for $i = 0, 1, \ldots, N = \dim(\mathcal{V}_h) =$ number of nodes in $\mathcal{T}_h$. Now substituting (6) and making some computations, we obtain:

$$\sum_{j=0}^{N} u_j \int_\Omega \gamma_\varepsilon \nabla\varphi_j \cdot \nabla\varphi_i \;=\; \oint_{\partial\Omega} g\varphi_i,$$

and we define $a_{ij} = \int_\Omega \gamma_\varepsilon \nabla\varphi_j \cdot \nabla\varphi_i$ and $f_i = \oint_{\partial\Omega} g\varphi_i$, we obtain a square linear equations system $\mathbf{Au} = \mathbf{f}$.

Similarly, replacing (6) into (5) we have

$$\sum_{j=0}^{N} u_j \oint_{\partial\Omega} \varphi_j \;=\; 0,$$

and we define $s_j = \oint_{\partial\Omega} \varphi_j$, we have a new constraint $\mathbf{s}^T\mathbf{u} = 0$ and with this we can obtain the final rectangular linear equations system

$$\mathcal{A}\mathbf{u} \;=\; \mathbf{b},$$

where $\mathcal{A}$ is a $(N+1) \times N$ matrix and $\mathbf{b} \in \mathbb{R}^{N+1}$ defined by

$$\mathcal{A} \;=\; \begin{bmatrix} \mathbf{A} \\ \mathbf{s}^T \end{bmatrix} \quad \text{and} \quad \mathbf{b} \;=\; \begin{bmatrix} \mathbf{f} \\ 0 \end{bmatrix}.$$

4. Implementation of FEM

In orden to implement a FEM scheme is necesary some modules like: polynomial basis functions φ_i, numerical quadratures, mesh or grid, etc. In figure 4, we present a scheme of implementation of the most important modules. In [7] and [2] you can see more computational aspects for a general FEM scheme.

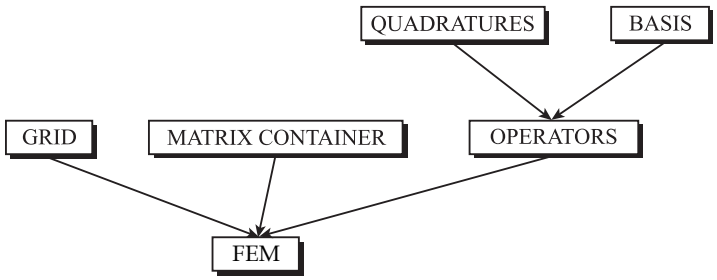

Figure 4: General scheme for a finite element implementation

In $\mathcal{T}_h$ we only going to consider the cells equivalent by a linear or affine transformation to a fixed cell called reference cell. In our case, the unit triangle was taken as a reference cell.

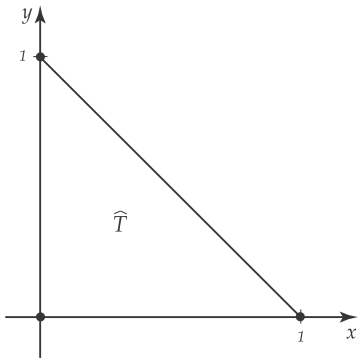

Figure 5: 2D Reference cell

In other words, we denoted by $\hat{T}$ the reference cell for each cell $T_k \in \mathcal{T}_h$, and there is an affine mapping $\phi_k(\hat{x}) = \mathcal{J}_k\hat{x} + b$ such that $\phi_k(\hat{T}) = T_k$ where $\mathcal{J}_k$ is the Jacobian of ϕ_k and holds that $|\mathcal{J}_k| = \det(\mathcal{J}_k) > 0$ for all $T_k \in \mathcal{T}_h$. Most of the calculations, especially those involving integration are performed in $\hat{T}$ and then through the Jacobian $\mathcal{J}_k$ of the function ϕ_k are mapped to the cell T_k.

Now consider $\hat{\Phi} = \{\hat{\varphi}_i\}$ a local basis for $\hat{T}$ and note that $\varphi_i^k = \hat{\varphi}_i \circ \phi_k^{-1}$ as appears in figure 6, where φ_i^k is the local basis for T_k.

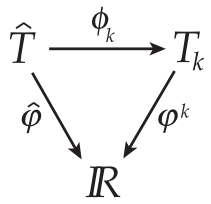

Figure 6: Construction of a basis in T_k from a basis in $\hat{T}$

4.1. Assemble the stiffness matrix

Consider N_T the number of cells in $\mathcal{T}_h$ and we have the entries for the stiffness matrix $\mathbf{A}$ are defined by

$$a_{ij} \;=\; \int_\Omega \gamma_\varepsilon \nabla\varphi_j \cdot \nabla\varphi_i \;=\; \sum_{k=0}^{N_T} \int_{T_k} \gamma_\varepsilon^k \nabla\varphi_j^k \cdot \nabla\varphi_i^k,$$

and applying the affine mapping ϕ_k we have

$$a_{ij} \;=\; \sum_{k=0}^{N_T} |\mathcal{J}_k| \int_{\hat{T}} \left(\gamma_\varepsilon^k \circ \phi_k^{-1}\right) \nabla\left(\hat{\varphi}_j \circ \phi_k^{-1}\right) \cdot \nabla\left(\hat{\varphi}_i \circ \phi_k^{-1}\right).$$

Later, for chain's rule we have

$$\nabla\left(\hat{\varphi}_i \circ \phi_k^{-1}\right) \;=\; \nabla\hat{\varphi}_i \cdot \nabla\phi_k^{-1},$$

where $\nabla\phi_k^{-1} = \mathcal{J}_k^{-1}$ and

$$\mathcal{J}_k^{-1} \;=\; \begin{bmatrix} \partial_x\hat{x} & \partial_y\hat{x} \\ \partial_x\hat{y} & \partial_y\hat{y} \end{bmatrix}.$$

Thus, we only compute a local contribution of $\mathbf{A}$ cell by cell. And for compute the integral on $\hat{T}$ you can use a quadrature for polynomials of dregee one, for example in this work we use:

$$\int_{\hat{T}} f(x_1, x_2) \;=\; \frac{1}{6}\Big[f(0,0) + f(1,0) + f(0,1)\Big].$$

4.2. Obtain additional constraint and source vector

We need to compute the vectors

$$\mathbf{f} \;=\; \left[\oint_{\partial\Omega} g\varphi_i\right] \quad \text{and} \quad \mathbf{s} \;=\; \left[\oint_{\partial\Omega} \varphi_i\right].$$

The way to compute both is the same, first note that

$$\oint_{\partial\Omega} g\varphi_i \;=\; \sum_{j=0}^{N_B} \oint_{e_j} g\varphi_i,$$

where N_B is the number of boundary edges in $\mathcal{T}_h$. Similarly to the assemble the stiffness matrix, we compute the contribution of the boundary edge e_j to the vector $\mathbf{f}$ and $\mathbf{s}$, this is easy to compute as a line integral in $[0,1]$,

$$\oint_{e_j} f \;=\; \int_0^1 f(\mathbf{r}(t)) \cdot |\mathbf{r}'(t)|\, dt,$$

and later compute the integral of $[0,1]$ with the Simpson's rule [8],

$$\int_0^1 f(x)\, dx \;\approx\; \frac{1}{6}\left[f(0) + 4f\left(\frac{1}{2}\right) + f(1)\right].$$

5. Implementation of the defect's detector

Now that we are able to obtain an approximation of u_ε from de problem (1), with FEM, we are going to solve the system (3) in order to obtain the position of D. For simplifying the presentation, we fix $\Omega = (0,1)\times(0,1)$, and thus, we need to compute the six values of

$$\Gamma_{ij} \;:=\; \int_{\partial\Omega} u_\varepsilon^{(i)} \gamma_0 \frac{\partial w^{(j)}}{\partial \nu} d\sigma - \int_{\partial\Omega} g^{(i)} w^{(j)} d\sigma,$$

where $g^{(1)}(x_1,x_2) = \begin{cases} -\gamma_0 & \text{if } x_1 = 0, \\ \gamma_0 & \text{if } x_1 = 1, \\ 0 & \text{otherwise} \end{cases}$, $g^{(2)}(x_1,x_2) = \begin{cases} -\gamma_0 & \text{if } x_2 = 0, \\ \gamma_0 & \text{if } x_2 = 1, \\ 0 & \text{otherwise} \end{cases}$, $u_\varepsilon^{(1)}$ is computed for (1) usind $g = g^{(1)}$, $u_\varepsilon^{(2)}$ usind $g = g^{(2)}$ and

$$w^{(1)}(x_1,x_2)=x_1 \qquad \frac{\partial w^{(1)}}{\partial \nu}=\begin{cases}-1 & \text{if } x_1=0\\ 1 & \text{if } x_1=1\\ 0 & \text{otherwise}\end{cases}$$

$$w^{(2)}(x_1,x_2)=x_2 \qquad \frac{\partial w^{(2)}}{\partial \nu}=\begin{cases}-1 & \text{if } x_2=0\\ 1 & \text{if } x_2=1\\ 0 & \text{otherwise}\end{cases}$$

$$w^{(3)}(x_1,x_2)=x_1x_2 \qquad \frac{\partial w^{(3)}}{\partial \nu}=\begin{cases}-x_2 & \text{if } x_1=0\\ x_2 & \text{if } x_1=1\\ -x_1 & \text{if } x_2=0\\ x_1 & \text{if } x_2=1\end{cases}$$

With this values and using the same technique that was used to computed the additional constraint and source vector, we can compute the values of Γ_{ij}, $i=1,2$ and $j=1,2,3$. Later, we solve the system (3) using Gaussian elimination or the Cramer's rule.

6. Numerical computations

For simplifying the presentation, we fix $\Omega=(0,1)\times(0,1)$, and consider that B is the unit ball (for the infinity norm) centered at the origin. We also set $z=\left(\frac{1}{2},\frac{1}{2}\right)^T$, $\varepsilon=0.1$, $\gamma_0=1$ and $\gamma_1=3$. All implementation and illustrations are performed with `FreeFem++` and `Scilab`.

Now, we used `FreeFem++` for computing an approximation of u_ε with P1 finite elements and a mesh size equal to 0.01, when g is the current corresponding to the background potential $u_0(x_1,x_2)=x_1$ and $u_0(x_1,x_2)=x_2$, and we obtain the results in figure 8.

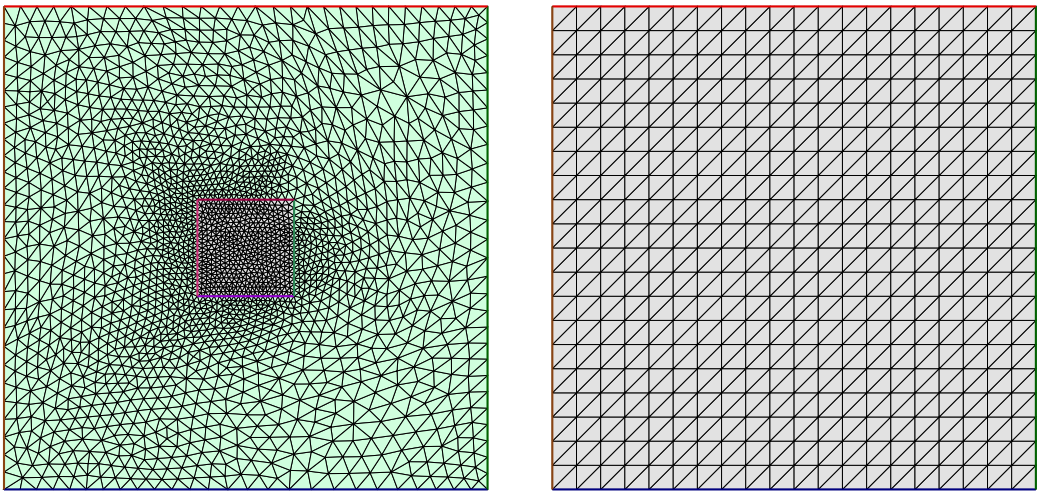

Figure 7: Unstructural mesh (left) and Cartesian mesh (right)

The mesh was constructed in `FreeFem++` and all the computations were in `Scilab`, i.e, from a conforming mesh obtained from `FreeFem++`, we implemented a `Scilab` code for

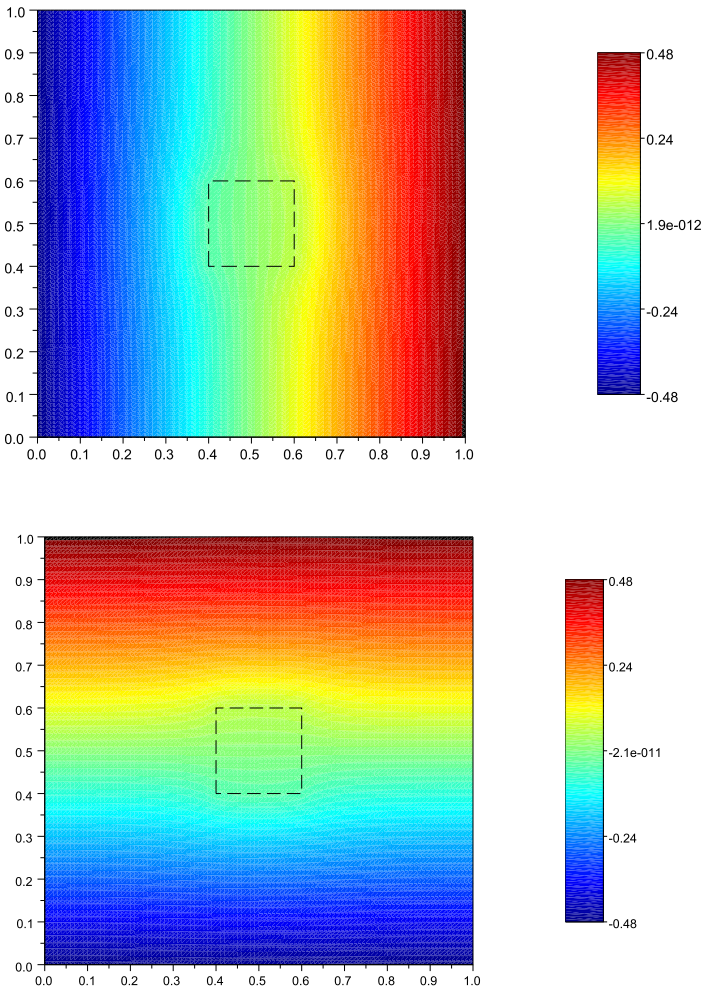

Figure 8: Approximarion for $u_\varepsilon^{(1)}$ (above) and for $u_\varepsilon^{(2)}$ (below)

computing an approximation of u_ε with $p = 1$ finite elements by using the Simpson formula for line integrals. With this code, we obtained a very good accuracy approximation of z.

7. Conclusion

The EIT techniques are new methods that have the advantage of being less invasive than mammography, but they are not used as a primary method, but rather as a complement to medical diagnosis. In our work, we verify that it is an effective technique to locate small imperfections quickly and only using domain information. In terms of implementation, we requires an efficient way of assembling the sparse matrix.

8. Acknowledgements

The authors would like to thank S. Mefire, B. Pinçon at the Institut Élie Cartan Nancy (IECN) and G. Sadaka at the Université de Picardie Jules Verne for their big help in this work. All the authors thank the M. Raydan, J.P. Chehab and the local and CIMPA organizing committee for the opportunity to participate in this research school.

References

[1] H. Ammari, S. Moskow and M.S. Vogelius, *Boundary integral formulas for the reconstruction of electromagnetic imperfections of small diameter*, ESAIM Control Optim. Calc. Var., 9 (2003), 49-66.

[2] P. E. Castillo and F. A. Sequeira, *Computational aspects of the LDG method on unstructured grids in 3D*, Mathematical and Computer Modelling (August 2011), doi:10.1016/j.mcm.2011.07.032.

[3] D.S. Holder, *Electrical Impedance Tomography: Methods, History and Applications*, Institute of Physics, 2004.

[4] C. Johnson, *Numerical Solution of Partial Differential Equations by the Finite Element Method*, Dover Publications, 2009.

[5] B. Pinçon, *An introduction to scilab for numerical simulations*, Institut Elie Cartan Nancy, 2012.

[6] G. Sadaka, `FreeFem++` *a tool to solve PDEs numerically*, Université de Picardie Jules Verne, 2012.

[7] F. Sequeira, *Aspectos computacionales del método Local Discontinuous Galerkin para mallas no estructuradas en 3D*, Master's Thesis, University of Puerto Rico at Mayag uez, 2010.

[8] E. Süli and D.F. Mayers, *An Introduction to Numerical Analysis*, Cambridge University Press, 2003.